

福島県立医科大学 学術機関リポジトリ



Title	Traffic of infused bone marrow cells after genetically-labeled syngeneic bone marrow transplantation following lethal irradiation in mice
Author(s)	Satoh, Atai; Saito, Takuro; Sato, Yoshihiro; Tsuchiya, Takao; Kenjo, Akira; Kimura, Takashi; Kanno, Ryuzo; Suzuki, Hiroyuki; Kogure, Michio; Hoshino, Yutaka; Gotoh, Mitsukazu
Citation	Fukushima Journal of Medical Science. 54(1): 11-24
Issue Date	2008-06
URL	http://ir.fmu.ac.jp/dspace/handle/123456789/221
Rights	© 2008 The Fukushima Society of Medical Science
DOI	10.5387/fms.54.11
Text Version	publisher

This document is downloaded at: 2024-04-25T00:19:26Z

TRAFFIC OF INFUSED BONE MARROW CELLS AFTER GENETICALLY-LABELED SYNGENEIC BONE MARROW TRANSPLANTATION FOLLOWING LETHAL IRRADIATION IN MICE

ATAI SATOH, TAKURO SAITO, YOSHIHIRO SATO, TAKAO TSUCHIYA,
AKIRA KENJO, TAKASHI KIMURA, RYUZO KANNO, HIROYUKI SUZUKI,
MICHIO KOGURE, YUTAKA HOSHINO and MITSUKAZU GOTOH

Department of Surgery I, Fukushima Medical University, School of Medicine, Fukushima, 960-1295, Japan

(Received November 14, 2007, accepted February 8, 2008)

Abstract: Bone marrow (BM) cells are considered the source of stem cells for various organs. However, how quickly BM cells can penetrate and constitute lymphoid organs remains elusive. In the present study, we addressed this issue in a model using genetically-labeled syngeneic BM transplantation (BMT).

Methods: Donor BM cells were obtained from "green mice", transgenic mice with enhanced GFP. Lethally irradiated C57BL/6 mice were infused with 1×10^6 BM cells from the green mice through the tail vein. BM chimerism was analyzed by FACS and the presence of donor BM cells in thoracoabdominal organs was assessed by fluorescence microscopy. The commitment of BM cells was examined by immunohistochemical staining using epithelium-, macrophage-, B and T-lymphocyte, and endothelium-specific antibodies.

Results: BM chimerism reached $40 \pm 18.5\%$, $82.6 \pm 23.4\%$, and $72 \pm 18\%$ (mean \pm SD) at 1, 4, and 12 wks after BMT, respectively. GFP-positive cells were detected in all organs in the course of chimeric formation. Most GFP-positive cells were T and B lymphocytes in lymphoid systems including spleen, thymus, mesenteric lymph nodes and microvilli, and some were positive for macrophage and endothelial cell markers.

Conclusions: Our results indicate that BM-derived cells migrate rapidly into various thoracoabdominal organs after BMT, and that lymphoid tissues are predominantly replaced with infused BM in lethally-irradiated mice. This confirmed the previous finding by others and suggests high interest of this model for further studies to characterize kinetics and roles of infused cells.

佐藤 直, 斎藤拓朗, 佐藤佳宏, 土屋貴男, 見城 明, 木村 隆, 管野隆三, 鈴木弘行, 木暮道彦,
星野 豊, 後藤満一

Corresponding author: Mitsukazu Gotoh, M.D., Ph.D E-mail: mgotoh@fmu.ac.jp

Abbreviations : BMT (bone marrow transplantation), BM (bone marrow), GFP (green fluorescent protein)

<http://www.fmu.ac.jp/home/lib/F-igaku/>

<http://www.sasappa.co.jp/online/>

Key words : Bone marrow transplantation, chimerism, green mouse, green fluorescent protein, lymphoid organ

INTRODUCTION

Recent studies on stem cells have suggested that the BM has cells with the potential to differentiate into mature cells of various organs including the heart, liver, kidney, lungs, gastrointestinal (GI) tract, skin, bone, muscle, cartilage, fat, endothelium, and brain, in addition to hematopoietic stem cells and supportive stromal cells¹⁾.

However, the developmental plasticity of adult hematopoietic stem cells to various organs is reported to be less than expected, and transdifferentiation may not be a general phenomenon, but rather may depend on the experimental system in which the hypothesis is tested²⁾.

Meanwhile, human BMT has gained widespread acceptance for the treatment of various hematological and neoplastic diseases³⁾. However, the procedures involved yield significant morbidity and mortality due to protracted and severe alterations in host immunological function before successful reconstitution^{3,4)}. Although hematopoietic cells are quickly restored and leukocyte numbers return to normal levels within a couple of weeks^{5,6)}, immune responses to various antigens^{6,7)} are usually distorted for a longer period of time⁶⁾. This may result from irradiation injury to lymphoid tissue as well as insufficient repopulation of atrophic lymphoid tissue following the modalities used before transplantation, however, the exact role of infused BM cells for these tissues has yet to be clearly determined^{2,3)}.

In the present study, we investigated the fate of infused syngeneic BM cells⁷⁾ that might repopulate lymphoid organs and also be involved in the replacement of parenchymal cells in various animal organs after lethal irradiation. BM cells from mice transgenic for GFP were used for the purpose of this analysis⁷⁾. The results confirm the previous findings by Weissman *et al.*²⁾ who showed little evidence for developmental plasticity of hematopoietic stem cells, and visualized rapid reconstitution of the peripheral lymphoid organs, suggesting efficacy of this model for further studies to characterize kinetics and roles of infused cells.

MATERIALS AND METHODS

Animals

Adult female C57BL/6 mice purchased from Charles River Japan (Tokyo, Japan) were used as recipients. GFP transgenic mice of C57BL/6 background were kindly provided by Dr Okabe (Research Institute for Microbial Diseases, Osaka University, Suita, Japan) and maintained in our animal facility⁷⁾. Male GFP mice aged 6-8 wks^{8,9)} were used as BM donors. GFP-mice are transgenic mouse lines

with enhanced GFP cDNA under the control of a chicken beta-actin promoter and cytomegalovirus enhancer⁵⁾. All of the tissues from these transgenic mice, with the exception of erythrocytes and hair, were green under excitation light. The experimental protocol was approved by the Ethics Review Committee for Animal Experimentation of Fukushima Medical University.

Preparation of GFP-chimeric mice

B6 mice were irradiated with X-ray at a dose of 7.5 ($n=4$), 9.5 ($n=4$), or 12 ($n=11$) Gy in order to examine the lethal dose. BM cells from GFP mice were collected by flushing the bone shafts of the femora with RPMI medium 1640 supplemented with 10% fetal calf serum. The cells were then washed once in this medium and suspended in phosphate-buffered saline (PBS) at doses of 10^5 , 10^6 , or 10^7 cells/mouse and injected via the tail vein.

Determination of bone-marrow-derived cell distribution in various organs

Chimeric animals were sacrificed at 1, 4, and 12 wks after BMT. Mice were anesthetized with ether, and systemic perfusion was established with 20 ml of 4% paraformaldehyde in PBS through the left ventricle after drawing blood from VCI. The lung, liver, pancreas, small intestines, kidneys and lymphoid organs including thymus, spleen and mesenteric lymph nodes were obtained for detection of BM-derived cells. BM cells were also obtained from the femur and examined for assessment of the chimeric rate.

Fluorescence-activated cell sorter (FACS) analysis 110

GFP-positive cells in peripheral blood cells, BM, and spleen were analyzed by flow cytometry using a FACS Calibur cell sorter (Becton-Dickinson, Mountain View, CA) equipped with a 530-nm filter at a bandwidth of +15 nm (Fig. 1).

Detection of GFP-positive cells and immunohistological studies

After sacrifice, parenchymal and lymphoid organs were collected and divided into two groups; one for frozen sections and one for paraffin sections. Tissue for the frozen sections was cut in 5-mm slices, embedded in Tissue Tek Compound, and frozen at -80°C. Tissue for the paraffin section was fixed overnight in 4% paraformaldehyde in PBS and dehydrated using 10%, 20%, and 30% sucrose solution overnight at 4°C and 120 then processed for paraffin sections.

Frozen sections of various organs were cut at 6- μ m thickness and examined under a fluorescence microscope for detection of GFP-positive cells. The fluorescence intensity of cells from B6 and GFP mice was used as negative and positive controls, respectively. Primary antibodies used for paraformaldehyde fixed paraffin-embedded sections were as follows, goat anti-mouse GFP antibody (1 : 100 dilution, Santa Cruz Biotechnology, Santa Cruz, CA), rabbit anti-human cytokeratin polyclonal antibody cross-reactive with mouse cytokeratin (1 : 700 dilution, DAKO,

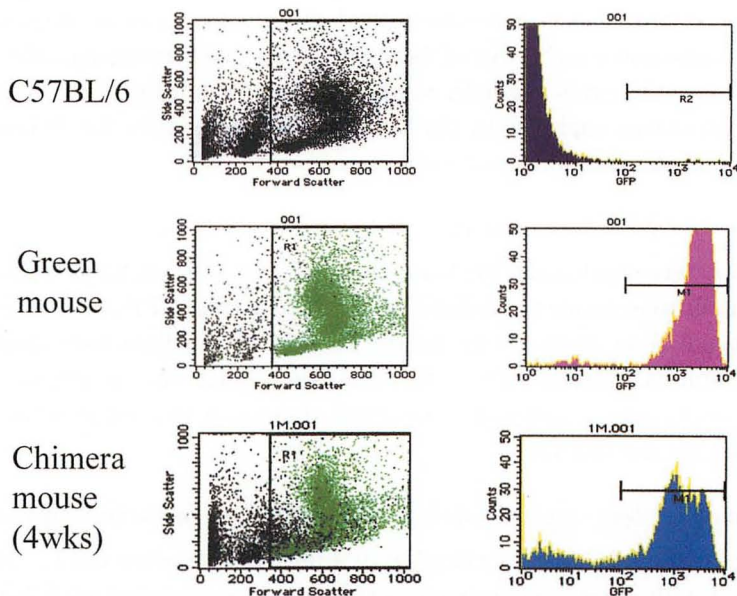


Fig. 1. FACS analysis of BM cells in a chimeric mouse after genetically-labeled syngeneic (green mouse) BM transplantation following lethal irradiation. The forward scatter was gated to obtain $97.4 \pm 1.1\%$ of GFP-positive cells in BM of green mice, but no cells in those of C57BL/6 mice.

Carpinteria, CA), biotin-conjugated rat anti-mouse F4/80 obtained from Serotec (1 : 5 dilution, Oxford, UK), rabbit anti-factor VIII related antigen (1 : 1 dilution, Zymed laboratories, San Francisco, CA), rabbit anti-human CD3 polyclonal antibody (1 : 100 dilution, DAKO), and rat anti-mouse CD45R/B220 monoclonal antibody (1 : 50 dilution, BD Biosciences Pharmingen, San Diego, CA). Secondary antibodies for each primary antibody were as follows; peroxidase-conjugated anti-goat rabbit immunoglobulin (Dako, Glostrup, Denmark) used for staining of GFP, biotin-conjugated anti-rabbit IgG (1 : 200 dilution, 135 Nichirei, Tokyo, Japan) used for cytokeratin, factor VIII and CD3, horseradish peroxidase conjugated streptavidin (Nichirei) used for F4/80, and peroxidase-conjugated rabbit anti-rat immunoglobulin IgG (DAKO) used for CD45R/B220. Sections of paraformaldehyde-fixed TISSUE-TEK mounted livers were stained with immunofluorescent technique using the same primary antibodies as paraformaldehyde-fixed paraffin-embedded sections. Cytokeratin, Factor VIII and F4/80 were visualized with rhodamine-conjugated tyramide (Perkin-Elmer Life Science, Boston, MA). CD3 and CD45R/B220 were visualized by Alexa Fluor 555 F(ab')2 fragment of goat anti-rabbit IgG (H+L) (Molecular Probes, Eugene, OR), and -labeled affinity purified antibody to Rat (H+L) (KPL Europe, Guildford, UK).

Fluorescence images were examined under a fluorescence microscope (ECLIPSE E800, Nikon, Japan) with excitation wave lengths of 460–500 nm for GFP and 510–560 nm for Alexa Fluor and rhodamine. Digital images captured by DXM 1200

(Nikon, Japan) were merged using Adobe Photoshop Elements 2.0.

Statistical analysis

All data were expressed as mean \pm SEM. Differences between groups were examined for statistical significance using the Student's *t*-test. A *P* value less than 0.05 denoted the presence of a statistically significant difference.

RESULTS

Irradiation dose and number of infused cells to establish long-term chimeric mice

Twelve Gy was selected as a lethal dose since 10 out of 11 mice died within two wks of this dose of irradiation, while none of animals died with 7.5 or 9.5 Gy. The 4-wks survival rates of mice injected with 10^5 , 10^6 , and 10^7 cells/mouse of BM cells were 70% (7/10), 100% (7/7), and 91% (10/11), respectively (Fig. 2a). BM cells harvested from mice given 10^5 , 10^6 , and 10^7 BM cells at 1 week after BMT showed a 160 dose-dependent increase in number (0.3 ± 0.3 , 1.5 ± 0.6 , and $2.7\pm0.6\times10^7$ cells, respectively), although those at 4 wks after BMT were not significantly different between the groups (4.0 ± 0.8 , 4.0 ± 1.3 , and $3.5\pm1.8\times10^7$, respectively) (Fig. 2b). Considering the values of control mice ($4.4\pm1.5\times10^7$), normal cell numbers in the BM were restored within 4 wks. Chimeric state at 4 wks after BMT reached the level of over 80% when either 10^6 or 10^7 BM cells were infused (84.2 ± 18.0 , $87.2\pm10.5\%$). As either dose maintained high chimeric state at 12 wks after BMT, 10^6 BM cells was selected as a dose to prepare chimeric mice for further experiments.

BM repopulation and GFP-positive cell ratio in peripheral blood, BM, and spleen

The proportions of GFP-positive cells in BM cells at 1, 4, and 12 wks after BMT were 35.2 ± 18.5 , 84.2 ± 18.0 , $72.0\pm18.0\%$, respectively (Fig. 2c). Those of spleen cells were 23.5 ± 12.8 , 66.2 ± 27.4 , $79.9\pm8.5\%$, respectively, and those of peripheral blood were 6.3 ± 6.4 , 83.4 ± 17.9 , $70.3\pm24.3\%$, respectively. Considering the proportion of GFP-positive cells in peripheral blood, BM, and spleen of green mice (86.5 ± 3.3 , 97.4 ± 1.1 , and 90.7 ± 11.5 , respectively), a high chimeric state was completed 4 wks after BMT and maintained for at least 12 wks.

BM-derived cells in various parenchymal and lymphoid organs at 12 wks after BMT by fluorescence microscopy

GFP-positive cells were found scattered or in some parts forming clumps in the lung, liver, pancreas, kidney, and small intestine. In contrast, GFP-positive cells were dominant in lymphoid organs including the spleen, thymus, and mesenteric lymph nodes (Fig. 3). One week after BMT, GFP-positive cells were detected in the lung, liver, kidney, and small intestine, but not in the pancreas. Four and 12 wks after BMT, GFP-positive cells increased in number and were detected in all organs. The numbers of cells migrating into these organs observed under a high power field

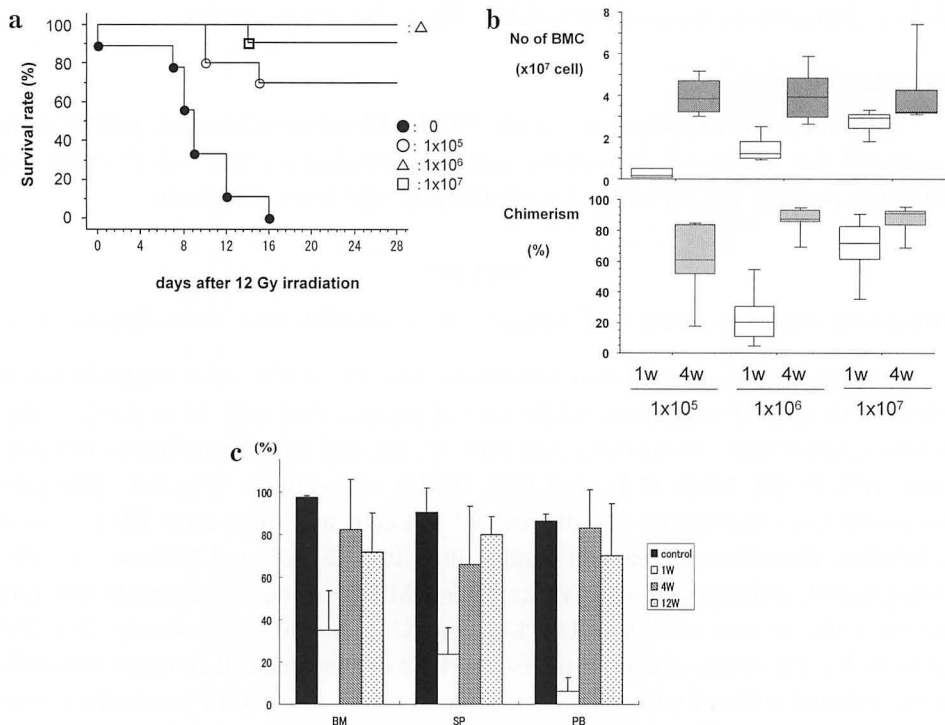


Fig. 2. (a) : Survival rate of animals given 12 Gy irradiation and various number of genetically-labeled syngeneic BM cells from green mice. (b) : Number of BM cells and rates of chimerism at 1 and 4 wks after various number of BMT. (C) : Proportion of GFP-positive cells in control and test animals transplanted with 1×10^6 BM cells from green mice after 12 Gy irradiation in BM, spleen (SP), and peripheral blood (PB). Data are shown as mean \pm SD of proportion of GFP-positive cells.

($\times 200$) at 4 and 12 wks after BMT were 10 ± 10 and 396 ± 98 cells in the lung, 4 ± 2 and 102 ± 36 cells in the liver, 0 and 56 ± 27 cells in the pancreas, 14 ± 9 and 210 ± 107 cells in the small intestine, and 0.6 ± 0.5 , 103 ± 23 cells in the kidney, respectively.

BM-derived cells in various parenchymal organs at 12 wks after BMT

Most of the mononuclear cells and some cells in the vessels of all organs studied were GFP-positive. GFP-positive cells in specific components of various organs were typical. In the lung, GFP-positive cells were found in the interstitial space but not in peripheral alveoli or bronchioles (Fig. 4a). In the liver, positive cells were scattered diffusely within the lobule, especially along the sinusoids, and were observed also in the periportal area. No GFP-positive cells were observed in hepatocytes, hepatic arteries or central veins (Fig. 4b). In the pancreas, GFP-positive cells were found in the interstitial space and in acinar and islet components, but not in acinar or islet cells, although some appeared to be present in the pancreatic ducts (Fig. 4c). In the kidney, GFP-positive cells were found only in the interstitial space,

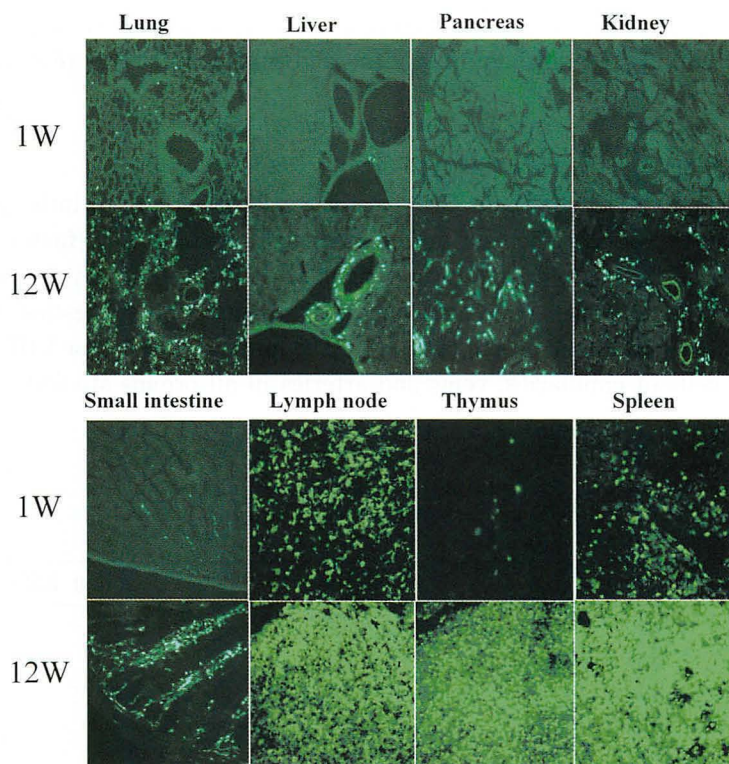


Fig. 3. BM-derived cells in various parenchyma and lymphoid organs at 1 and 12 wks after BMT. GFP-positive cells were found scattering in lung, liver, pancreas, kidney, small intestine and were dominant in lymphoid organs including spleen, thymus, and mesenteric lymph nodes on fluorescence microscope ($\times 200$).

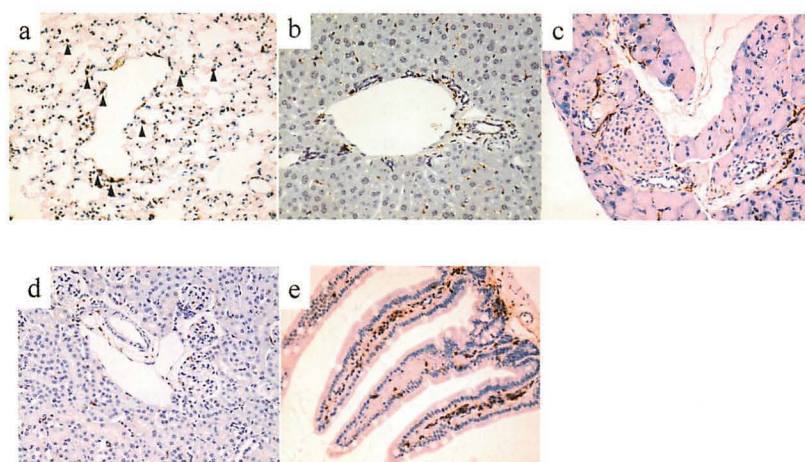


Fig. 4. BM derived GFP-positive cells in various parenchymal organs 12 wks after BMT (lung (a), liver (b), pancreas (c), kidney (d) and small intestine (e)) and cells recognized by the antibodies for GFP ($\times 200$).

but not in any glomeruli (Fig. 4d). In the small intestines, many GFP-positive cells were found within the villi (lamina propria) and submucosal layer (Fig. 4e).

Antibody specificities used in immunohistological studies and possible transdifferentiation of BM cells to specific cell types

To determine whether these GFP-positive cells differentiate into specific cell types, we used three different antibodies recognizing cytokeratin, factor VIII, and F4/80. The antibody for cytokeratin visualizes epithelial cells in the lung (bronchioles), liver (bile duct), pancreas (pancreatic duct), small intestine (intestinal epithelial cells), and kidney (renal tubules). The antibody for factor VIII visualizes endothelial cells of capillaries, veins and arteries in all organs studied. The anti-

Table 1. Percentages of GFP-positive cells in various components of thoracoabdominal organs at 4 and 12 wks after BMT

Organ/Structure	4 wks post-BMT	12 wks post-BMT
Liver		
Hepatocytes	0	0
Bile ducts	1.0(5/493)†	0.5(3/593)
Kupffer cells	50.1(400/798)	67.2(312/464)
Portal veins	5.5(10/180)	2.8(5/176)
Portal artery	0	0
Central vein	0	0
Small Intestine		
Epithelial cells	0.1(6/5372)	0.8(38/4576)
Endothelial cells	0.4(1/258)	0
Kidney		
Tubules	0	0
Collecting tubules	0	0
Glomeruli	0	0
Renal arteries	0	0
Renal veins	5.9(10/168)	1.5(3/201)
Lung		
Bronchi	0	0
Pulmonary artery	0	0
Pulmonary vein	0	4.6(14/304)
Pancreas		
Acinar cells	0	0
Pancreatic ducts	3.3(19/577)	0.1(1/708)
Islet	0	0
Pancreatic artery	0	0
Pancreatic vein	0	0.9(2/213)

#: Number of the respective marker positive cells/GFP-positive cells

body for F4/80 only visualized Kupffer cells in the liver.

Examination of serial sections with anti-GFP antibody and one of the antibodies for cytokeratin, factor VIII, or F4/80 indicated transdifferentiation of BM cells to specific cell types. Epithelial cells in the bile ducts, pancreatic ducts, and small intestines were double-positive for GFP and cytokeratin. Endothelial cells in veins of the lung, liver and small intestine were double-positive for GFP and factor VIII. Most Kupffer cells in the liver were double-positive for GFP and F4/80. GFP-positive cells in each organ studied were quantitatively examined in three mice and the results are summarized in Table 1.

BM-derived cells in various lymphoid organs

Irradiation induced atrophy of thymus and mesenteric lymph nodes. Histological study of the thymus failed to show discrete cortical and medullary regions with reduced numbers of thymocytes. A few GFP-positive cells were found (Fig. 5a). At 12 wks post-BMT, GFP-positive cells were found in the cortex as well as in medulla with numerous thymocytes (Fig. 5b). This was also the case with lymph nodes that showed restoration of typical lymph architecture consisting of medulla and paracortical areas at 12 wks post-BMT (Figs. 5c & d). In the spleen, most of the white pulps were replaced with GFP-positive cells at 12 wks post-BMT (Figs. 5e & f). As found in FACS analysis of splenocytes, the proportion of GFP-positive cells was 80% at 12 wks after BMT. Histological examination of other lymphoid organs including the thymus, mesenteric lymph nodes, and villi of small intestines revealed a similar pattern. Immunohistological examination of lymphoid tissue revealed that significant numbers of CD3-positive cells were GFP-positive in the merged images (Fig. 6). This was also the case with CD45R-positive cells within the spleen, lymph node, and villi of the small intestine (Fig. 7).

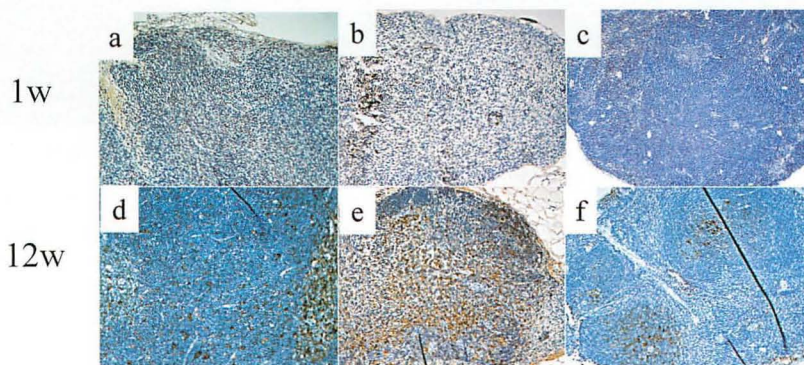


Fig. 5. GFP-positive cells in thymus (a, d), mesenteric lymph nodes (b, e) and spleen. (c, f) one and 12 wks after BMT. The number of these cells was increased at 12 wks after BMT and restoring original architectures of thymus and lymph nodes ($\times 100$).

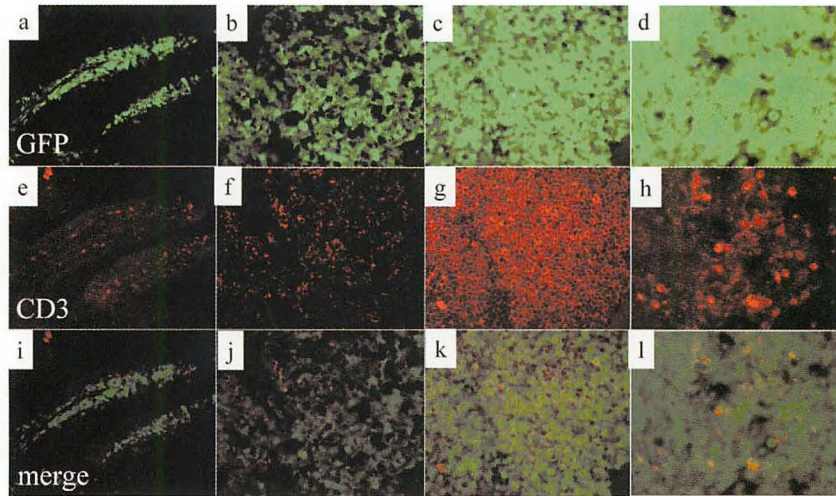


Fig. 6. BM derived GFP-positive, CD3 positive and double positive cells in various lymphoid organs on fluorescence microscopy. In small intestine (a, e, i: $\times 200$), lymph nodes (b, f, j: $\times 400$), thymus (c, g, k: $\times 400$) and spleen (d, h, l: $\times 400$), significant number of CD3 positive cells were noted having GFP when merged.

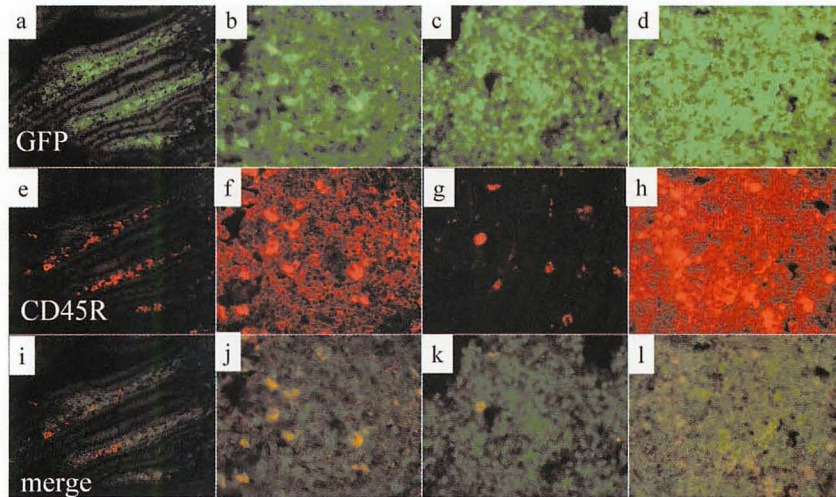


Fig. 7. BM derived GFP-positive, CD45R positive and double positive cells in various lymphoid organs on fluorescence microscopy. In small intestine (a, e, i: $\times 200$), lymph nodes (b, f, j: $\times 400$), thymus (c, g, k: $\times 400$) and spleen (d, h, l: $\times 400$), significant number of CD45R positive cells were noted having GFP when merged.

DISCUSSION

Syngeneic BM transplantation using green mice demonstrated the participation of BM cells in various parenchymal and lymphoid organs. We found that lymphoid organs were repopulated rather quickly consistent with BM repopulation to main-

tain peripheral blood cells after BMT. Significant numbers of Kupffer cells and endothelial cells in most of the organs were found to be BM-derived, while a few epithelial cells were found to be BM-derived.

The characteristic of this model was BM reconstitution after lethal irradiation, giving a model relevant to clinical BM transplantation. Animals could not survive and died several days after lethal irradiation without BM transplantation. X-ray irradiation was used for ablation of BM and to create space for infused BM cells as previously suggested by Tomita Y *et al.*³⁾. The chimeric state of BM was over 70-80% 12 wks after BMT. These animals could survive for more than one year without any obvious complications. Under lethal irradiation, traffic of infused BM cells to each organ was monitored and a marked difference was demonstrated between the lymphoid and parenchymal organs studied here.

Although significant numbers of BM cells were found to be scattered in various parenchymal organs including the lung, liver, pancreas, small intestines, and kidney, the antibody used to detect epithelial cells could visualize only a few cells in the respective organ. Epithelial cells in bile ducts, pancreatic ducts, and small intestines were GFP-positive. This was consistent with the observations by Krause and colleagues who showed that BM derived hematopoietic stem cells can transdifferentiate to epithelial cells in various organs¹⁾. However, we failed to detect BM-derived cells in renal tubules or the glomeruli.

In contrast to epithelial cells, transdifferentiation to endothelial cells recognized by anti-factor VIII was visualized frequently when compared to epithelial cells in all the organs studied here. It has been shown that endothelial progenitor cells first found in the peripheral blood⁸⁾ and BM origin of endothelial progenitor cells are responsible for postnatal vasculogenesis in physiological and pathological neovascularization⁹⁾. It was interesting to note that many BM-derived endothelial cells were found in the veins, but rarely in the arteries. The reason for this is unknown, but irradiation injury is thought to be a causative factor for differentiation of progenitor cells to endothelial cells. This is consistent with previous findings by others who showed that recruitment of BM-derived endothelial cells was observed to sites prominent components quickly repopulated with BM-derived cells where neovascularization takes place in liver¹⁰⁾ or pancreatic islets¹¹⁾.

Kupffer cells are replaced with BM cells of recipient origin in a rat liver transplantation model¹²⁾ and in human cases¹³⁾. On the contrary, following allogenic BM transplantation, Kupffer cells in the liver were predominantly of donor marrow origin by day 21 post-BMT¹⁴⁾. This was also the case with this syngeneic BM transplantation model in which two-thirds of Kupffer cells were replaced at 4 wks and most of Kupffer cells were replaced at 12 wks with donor-type cells. In our model, the liver and BM were irradiated with a lethal dose. Irradiation is reported to cause injury to hepatocytes as well as Kupffer cells¹⁵⁾ and this injury might enhance repopulation of Kupffer cells with infused BM cells.

The BMT procedure is associated with phenotypic changes in circulating

peripheral blood lymphocyte subsets, and a reduced ability of the host to produce immunoglobulin of various isotypes after antigen stimulation^{16,17)}. Deficits in various T cell-mediated functions, such as mitogen responsiveness, helper-cell function, cytotoxicity, and contact hypersensitivity have also been described. In addition, natural killer cell activity appears to be transiently depressed in BMT recipients¹⁸⁾. While some of these alterations in immune function reverse with time, others, such as helper T cell function, contact hypersensitivity, and IgA secretion, remain depressed for years after successful engraftment¹⁹⁾. In this study, we found that irradiation induced remarkable changes in the lymphoid organs, in particular the thymus and mesenteric lymph nodes. Thymus size was not completely restored at 12 wks post-BMT (0.023 ± 0.012 vs 0.07 ± 0.01 g of control, $n=3$), although the majority of T cells in lymphoid organs were found to be BM-derived. Mesenteric lymph nodes were quite atrophic at 1 week post irradiation, although they regained their size gradually, but not completely at 12 wks post-BMT (0.02 ± 0.010 vs 0.023 ± 0.006 g of control, $n=3$). This is consistent with the previous study by Samlowski and colleagues involving syngeneic murine BMT, who noted persistently hypoplastic peripheral lymph nodes in recipient mice for many months after successful transplantation²⁰⁾.

There are only a few clinical histological studies investigating lymphoid tissue post BMT^{21,22)}. Horny *et al.* reported severe atrophy of the lymphoreticular tissue with marked depletion of lymphocytes in four patients who died between 0.5 and 12 months after transplantation²¹⁾. However, interpretation needs careful consideration of the histological findings because of immunosuppression as well as phenomena related to graft-versus-host disease²¹⁾. Experimentally, only a few studies examined levels of reconstitution of infused BM cells to reconstruct lymphoid tissues after syngeneic BM transplantation, in which chimerism was mostly determined by FACS analysis^{23,24)}. In this study GFP-positive syngeneic BM cells clearly demonstrated steps of reconstitution of lymphoid organs. There were not many GFP-positive cells not at 1 week post infusion, however, these cells rapidly accumulated in the later period in lymphoid organs including the thymus, mesenteric lymph nodes, and spleen. These morphological changes might be explained by the finding of irradiation-induced anatomic change of high endothelial venules, which regulates entry of lymphocytes to lymphoid system²⁰⁾.

Although there is a possibility of fusion as a phenomenon which could account for the observations²⁵⁾, it is noteworthy that lymphoid tissues are predominantly replaced with infused BM in lethally-irradiated mice in contrast with less plasticity of the cells in non-lymphoid organs. Although detailed functional and histological assessment of these lymphoid organs needs to be evaluated in the future study, this model is simple and reproducible and would offer strategies to examine various techniques and modulations on speed of engraftment and distribution of donor cells in lymphoid organs after transplantation.

REFERENCES

1. Krause DS, Theise ND, Collector MI, Henegariu O, Hwang S, Gardner R, Neutzel S, Sharkis SJ. Multi-organ, multi-lineage engraftment by a single bone marrow-derived stem cell. *Cell*, **105** : 369-377, 2001.
2. Wagers AJ, Sherwood RI, Christensen JL, Weissman IL. Little evidence for developmental plasticity of adult hematopoietic stem cells. *Science*, **297** : 2256-2259, 2002.
3. Tomita Y, Sachs DH, Sykes M. Myelosuppressive conditioning is required to achieve engraftment of pluripotent stem cells contained in moderate doses of syngeneic bone marrow. *Blood*, **15** ; **83** : 939-948, 1994.
4. Wingard JR. Bone marrow to blood stem cells. Past, Present, Future. *In* : Whedon MB, Wujcik D, eds. *Blood and marrow stem cell transplantation*. Jones and Bartlett Publishers, Boston, 3-24, 1997.
5. Strohl RA. Radiation therapy in transplantation. *In* : Whedon MB, Wujcik D, eds. *Blood and marrow stem cell transplantation*. Jones and Bartlett Publishers, Boston, 151-161, 1997.
6. Frasca D, Guidi F, Arbitrio M, Pioli C, Poccia F, Cicconi R, Doria G. Hematopoietic reconstitution after lethal irradiation and bone marrow transplantation: effects of different hematopoietic cytokines on the recovery of thymus, spleen and blood cells. *Bone Marrow Transplant*, **25** : 427-433, 2000.
7. Okabe M, Yamamoto H. Green fluorescent protein-transgenic mice: immune functions and their application to studies of lymphocyte development. *Immunol Lett*, **70** : 165-171, 1999.
8. Asahara T, Murohara T, Sullivan A, Silver M, van der Zee R, Li T, Witzenbichler B, Schatteman G, Isner JM. Isolation of putative progenitor endothelial cells for angiogenesis. *Science*, **275** : 964-967, 1997.
9. Asahara T, Masuda H, Takhashi T, et al. Bone marrow origin of endothelial progenitor cells responsible for postnatal vasculogenesis in physiological and pathological neovascularization. *Circ Res*, **85** : 221-228, 1999.
10. Grompe M. The role of bone marrow stem cells in liver regeneration. *Semin Liver Dis*, **23** : 363-372, 2003.
11. Mathews V, Hanson PT, Ford E, Fujita J, Polonsky KS, Graubert TA. Recruitment of bone marrow-derived endothelial cells to sites of pancreatic beta-cell injury. *Diabetes*, **53** : 91-98, 2004.
12. Kubota N, Monden M, Hasuike Y, Valdivia LA, Gotoh M, Mori T, Onoue K, Wakasa K, Sakurai M. Lymphocyte infiltration and Ia expression in liver allografts in rats. *Transplant Proc*, **20** : 214-216, 1988.
13. Gouw AS, Houthoff HJ, Huitema S, Beelen JM, Gips CH, Poppema S. Expression of major histocompatibility complex antigens and replacement of donor cells by recipient ones in human liver grafts. *Transplantation*, **43** : 291-296, 1987.
14. Paradis K, Sharp HL, Vallera DA, Blazar BR. Kupffer cell engraftment across the major histocompatibility barrier in mice: bone marrow origin, class II antigen expression, and antigen-presenting capacity. *J Pediatr Gastroenterol Nutr*, **11** : 525-533, 1990.
15. Clement O, Muhler A, Vexler VS, Rosenau W, Berthezene Y, Kuwatsuru R, Brasch RC. Evaluation of radiation-induced liver injury with MR imaging: comparison of hepatocellular and reticuloendothelial contrast agents. *Radiology*, **185** : 163-168, 1992.
16. Armitage RJ, Goldstone AH, Richards JD, Cawley JC. Lymphocyte function after autologous bone marrow transplantation (BMT): a comparison with patients treated with allogeneic BMT and with chemotherapy only. *Br J Haematol*, **63** : 637-647, 1986.
17. Pan L, Bressler S, Cooke KR, Krenger W, Karandikar M, Ferrara JL. Long-term engraftment, graft-vs.-host disease, and immunologic reconstitution after experimental transplantation of allogeneic peripheral blood cells from G-CSF-treated donors. *Biol Blood Marrow Transplant*, **2** : 126-133, 1996.

18. Bengtsson M, Totterman TH, Smedmyr B, Festin R, Oberg G, Simonsson B. Regeneration of functional and activated NK and T sub-subset cells in the marrow and blood after autologous bone marrow transplantation: a prospective phenotypic study with 2/3-color FACS analysis. *Leukemia*, **3**: 68-75, 1989.
19. Zander AR, Reuben JM, Johnston D, Vellekoop L, Dicke KA, Yau JC, Hersh EM. Immune recovery following allogeneic bone marrow transplantation. *Transplantation*, **40**: 177-183, 1985.
20. Samlowski WE, Johnson HM, Hammond EH, Robertson BA, Daynes RA. Marrow ablative doses of gamma-irradiation and protracted changes in peripheral lymph node microvasculature of murine and human bone marrow transplant recipients. *Lab Invest*, **56**: 85-95, 1987.
21. Horny HP, Horst HA, Ehninger G, Kaiserling E. Lymph node morphology after allogeneic bone marrow transplantation for chronic myeloid leukemia: a histological and immunohistological study focusing on the phenotype of the recovering lymphoid cells. *Blut*, **57**: 31-40, 1988.
22. Miller SC. Hematopoietic reconstitution of irradiated, stem cell-injected mice: early dynamics of restoration of the cell lineages of the spleen and bone marrow. *J 405 Hematother Stem Cell Res*, **11**: 965-970, 2002.
23. Auletta JJ, Devecchio JL, Ferrara JL, Heinzel FP. Distinct phases in recovery of reconstituted innate cellular-mediated immunity after murine syngeneic bone marrow transplantation. *Biol Blood Marrow Transplant*, **10**: 834-847, 2004.
24. Janczewska S, Wisniewski M, Stepkowski SM, Lukomska B. Fast hematopoietic recovery after bone marrow engraftment needs physiological proximity of stromal and stem cells. *Cell Transplant*, **12**: 399-406, 2003.

Acknowledgement : This work was supported in part by grants from the Japanese Ministry of Education, Culture, Sports, Science and Technology and in part by Grant-in-Aid for Research on Human Genome, Tissue Engineering Food Biotechnology, Health Sciences Research Grants, Ministry of Health, Labor and Welfare of Japan.

The authors gratefully acknowledge Ms. Yukiko Kikuta and Ms. Kayoko Kobayashi for their invaluable assistance in the preparation of the figures and manuscript.